

# Backstepping Based Control of PV system Connected to the Grid

C. Aouadi\*, A. Abouloifa

LTI Lab. Faculty of Science Ben M'sik  
University HASSAN II Mohammedia-Casablanca  
Casablanca, Morocco

\*Email : aouadi.chaouki {at} gmail.com

A. Hamdoun, Y. Boussairi

LTI Lab. Faculty of Science Ben M'sik  
University HASSAN II Mohammedia-Casablanca  
Casablanca, Morocco

**Abstract**— This paper involves the nonlinear control of single phase grid connected photovoltaic system with LCL filter. The control objective is threefold i) extracting the maximum power from the PV array by acting on the DC/DC converter (MPPT) ii) providing a current with sinusoidal waveform and in phase with the grid voltage by means of controlling DC/AC converter (power factor correction: PFC) iii) regulating the DC voltage to a desired value (VR). The whole system is described by 5<sup>th</sup> order nonlinear mathematical model and controlled by using the backstepping approach and tools from Lyapunov stability. The simulation results have been performed through Matlab/Simulink environment and show that the designed controller meets its objective.

**Keywords**-PV array; averaging model; backstepping technique; Lyapunov stability; MPPT; PFC.

## I. INTRODUCTION

Since, the world demand for electricity increase very quickly, and the progress of the power electronic, the photovoltaic generation connected to the grid has obtained a great attention to meet the rising electricity demand. Solar energy is considered to be one of the most useful natural energy sources because it's free, and clean. In addition, the major advantage of the photovoltaic systems is to meets the basic power requirement of non-electrified remote areas, where grid power has not yet reached, also it can be used as a grid power sources for urban applications.

For PV power generation, it usually consists of an array of PV panels and adaptation circuit that consists on a power chopper, power inverter and some filter. The maximum power point of PV panels can be tracked by means of regulating the PV voltage tanks to the DC/DC converter. Over the years, different MPPT techniques have been proposed for PV power generation. These methods mainly include the perturbation and observation method (P&O) [1], the incremental conductance [2], the hill-climbing search and some other special methods, such as fuzzy logic technique, neural networks. The P&O MPPT algorithm is mostly used, due to its ease of implementation.

PV energy application can be divided into two parts: Stand-alone systems that require a battery to store the energy and the PV grid connected systems used in high power application.

The last system is gaining today the most interest over traditional stand-alone PV systems.

In order to eliminate the harmonics distortion of current and voltage and to optimize the active power flow between system power sources and the grid, many control methods are proposed in [3], [4], [5], [6]. Indeed, [7] proposed a passivity-based control, in [8], the Proportional Resonant (PR) controller and Multi Resonant Controllers (MRC) are developed. Besides the conventional methods, there are some more advanced control techniques like the genetic algorithms, the fuzzy logic and the artificial neural networks (ANNs) [9], which can readily incorporate human intelligence in complicated control systems.

In this work, we propose the nonlinear control of the PV system connected to the grid using backstepping approach and Lyapunov stability tools.

The content of this paper is outlined as follows. In section II, presentation of single phase grid connected. In the section III, a mathematic models of all system stage. In section IV, a controller design of the converters using a backstepping method. And the section V is devoted for simulation of the system with the conclusion.

## II. PRESENTATION OF SYSTEM

Figure 1 shows the system configuration of the proposed single phase grid connected to the photovoltaic array, this system consist of a solar array, a DC/DC boost chopper used to increasing the voltage level of photovoltaic array and to feed DC side of the inverter. The last provides the energy to the grid. The LCL filter is used in order to minimize the harmonics distortion of current and voltage.

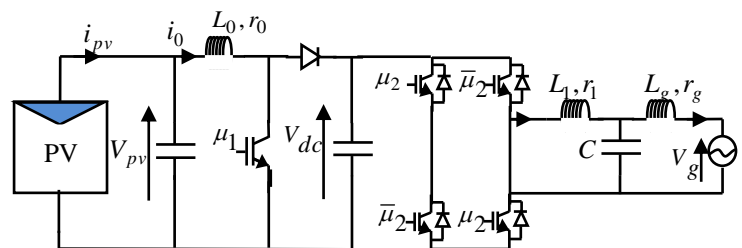


Fig.1: single phase grid connected to the PV module

### III. MATHEMATICAL MODEL

#### A. Modeling of PV array

Figure 2 shows the equivalent circuit of solar cell, it is formed by a photocurrent source, diode, parallel resistor  $R_p$ , and a series resistor  $R_s$ . Using Kirchhoff's current law, the photovoltaic current equation can be represented as follows [10]:

$$I = I_{ph} - I_0 \left( \exp\left(\frac{V + I R_s}{V_t}\right) - 1 \right) - \left( \frac{V + I R_s}{V_t} \right)$$

where  $I_{ph}$  and  $I_0$  are the light-generated current at the nominal condition (usually 1000W/m<sup>2</sup> and 25 °C) depend on the temperature and irradiance, and saturation current of the cell which can be described as:

$$I_{ph} = I_{sc} + K_i (T - T_{ref}) * G / 1000$$

$$I_0 = \frac{I_{sc} + K_i (T - T_{ref})}{\exp\left(\frac{V_{co} + K_v (T - T_{ref})}{n * V_t}\right) - 1}$$

$K_v$  : Is the open voltage/temperature coefficient.

$K_i$  : Is the short circuit current/temperature coefficient.

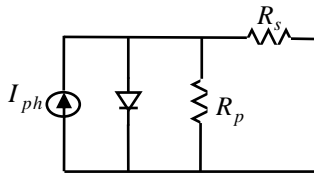


Fig.2: Equivalent circuit of solar cell

The PV array is a result of associating of  $N_s$  cells in series and  $N_p$  strings in parallel (each string has  $N_s$  cells series). In this case, the output current and voltage can be expressed as follows:

$$V_m = N_s * V_{cell}$$

$$I_m = N_p * I_{cell}$$

The terminal equation for current and voltage of the solar PV array is mentioned below as described by many authors ([11], [12]):

$$I_m = N_p I_{ph} - N_p I_0 \left( \exp\left(\frac{V_m + I_m \frac{N_s}{N_p} R_s}{V_t}\right) - 1 \right) - \frac{N_s}{N_p} \frac{R_s}{R_p} \frac{V_m + I_m \frac{N_s}{N_p} R_s}{V_t}$$

$v_t$  : Is the thermal voltage.

In this paper we use six modules in series to construct an array. Each module contained 54 cells connected in series. The table below represent the experimental parameters of the module, these parameters obtained from the datasheet of KC200GT.

Parameter	Value
Max Power	200.143 W
Short circuit current	8.21 A
Open circuit voltage	32.9 V
Max Power voltage	26.3
Max Power current	7.61 A
Num of parallel cells	1
Num of series cells	54

Table 1: PV modules paramters

#### B. Modeling of the inverter and the filter

A typical single-phase inverter has the structure shown in figure 3. It consists of a single-phase full-bridge where the switches can be IGBT or MOSFET. From the AC side, the converter is connected, in parallel with a grid through an LCL filter. The control input of the inverter takes the values in the set  $\{-1, 1\}$

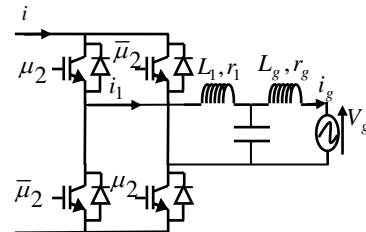


Fig.3: Single phase inverter and L-C-L filter

Applying the usual Kirchhoff's laws to the above circuit one gets:

$$L_1 \frac{di_1}{dt} = \mu_2 v_{dc} - v_c - r_1 i_1$$

$$L_g \frac{di_g}{dt} = v_c - v_g - r_g i_g$$

$$C \frac{dv_c}{dt} = i_1 - i_g$$

with  $i = \mu_2 * i_1$ . And  $i_{k1} = \frac{1 + \mu_2}{2} * i_1$  and  $i_{k2} = \frac{\mu_2 - 1}{2} * i_1$

the switching function of the inverter is defined as:

$$\mu_2 = \begin{cases} 1 & \text{if } (S_1, S_4) \text{ is ON and } (S_2, S_3) \text{ is OFF} \\ -1 & \text{if } (S_1, S_4) \text{ is OFF and } (S_2, S_3) \text{ is ON} \end{cases}$$

The obtained average model is the following:

$$L_g \dot{x}_1 = x_2 - v_g - r_g x_1 \tag{1}$$

$$C \dot{x}_2 = x_3 - x_1 \tag{2}$$

$$L_1 \dot{x}_3 = u_2 x_6 - x_2 - r_1 x_3 \tag{3}$$

where  $x_1, x_2, x_3$  and  $u_2$  denote the average values, over cutting periods, of the signals  $i_1, i_g, v_g$  and  $\mu_2$ . In the system (1-3) the mean value  $u_2$  of  $\mu_2$  turns out to be the system control input.

C. Boost converter modelling

Figure 4 shows the basic circuit configuration of a boost converter. The equations that represent the instantaneous model of the converter during the cutting period  $T$  are the following:

$$C_{pv} \frac{dv_{pv}}{dt} = i_{pv} - i_0$$

$$L_0 \frac{di_0}{dt} = v_{pv} - (1 - \mu_1)v_{dc} - r_0 i_0$$

$$C_{dc} \frac{dv_{dc}}{dt} = (1 - \mu_1)i_0 - \mu_2 i_1$$

The average model is the following:

$$C_{pv} \dot{x}_4 = i_{pv} - x_5 \tag{4}$$

$$L_0 \dot{x}_5 = v_{pv} - (1 - u_1)x_6 - r_0 x_5 \tag{5}$$

$$C_{dc} \dot{x}_6 = (1 - u_1)x_5 - u_2 x_3 \tag{6}$$

where  $x_4, x_5, x_6$  and  $u_1$  denote the average values, of the signals  $v_{pv}, i_0, v_{dc}$  and  $\mu_1$ .

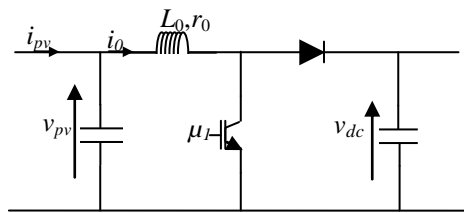


Fig.4: Boost converter

IV. BACKSTEPPING CONTROLLER DESIGN

The aim of this section is to design a controller that will be able to ensure: (i) global stability of the system, (ii) Power factor correction in the grid side, (iii) perfect MPPT, and (iv) DC bus voltage regulation. Figure 5 shows the structure of whole controlled system

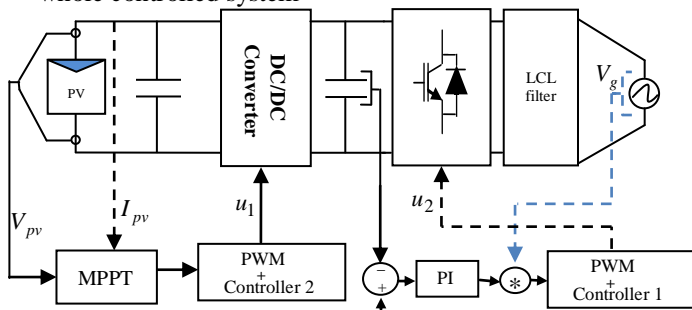


Fig.5: PV system with multiple controllers

A. PFC controller

The PFC objective means that the grid current  $i_g$  should be sinusoidal and in phase with the grid voltage  $v_g$ , therefore, the

aim is to directly enforce the current  $x_1$  to track a given reference current  $x_1^*$  of the form  $x_1^* = \beta v_g$  where  $\beta$  is a real signal to be defined later. Following the backstepping approach, a controller is designed in three steps based on the model (1-3), because the controlled system has the relative degree equal three with respect to the output signal  $x_1$ .

Step 1

Let us introduce the following current error:

$$z_1 = L_g(x_1 - x_1^*)$$

where  $x_1^*$  denotes the corresponding reference signal. Using (1), time derivation of  $z_1$  yields the error dynamics:

$$\dot{z}_1 = x_2 - v_g - r_g x_1 - L_2 \dot{x}_1^* \tag{7}$$

Consider the following candidate Lyapunov function:

$$V_1 = 0.5 z_1^2 \tag{8}$$

Its time derivative is given by:

$$\dot{V}_1 = z_1 \dot{z}_1 \tag{9}$$

The choice  $\dot{z}_1 = -c_1 z_1$  lead us  $\dot{V}_1 = -c_1 z_1^2$  and consequently the system is globally asymptotically stable ( $c_1$  is a positive design parameter).

Using  $\dot{z}_1 = -c_1 z_1$  and equation (7), one has:

$$x_2 - v_g - r_g x_1 - L_2 \dot{x}_1^* = -c_1 z_1$$

In the above equation, if we choice  $x_2$  as a virtual control variable ( $x_2 = x_2^*$ ) so, we can find the following stabilizing function:

$$x_2^* = -c_1 z_1 + v_g + L_g \dot{x}_1^* + r_g x_1 \tag{10}$$

As  $x_2^*$  is not the actual control input, a new error variable  $z_2$ , between the virtual control and its desired value  $x_2^*$ , is introduced:

$$z_2 = C(x_2 - x_2^*) \tag{11}$$

Using (10) and (11), equations (7) and (9) become:

$$\dot{z}_1 = \frac{z_2}{C} - C_1 z_1$$

$$\dot{V} = \frac{z_1 z_2}{C} - c_1 z_1^2$$

**Step 2:**

Using equation (2), Time derivation of  $Z_2$  is given by:

$$\dot{z}_2 = x_3 - x_1 - C \dot{x}_2^* \quad (12)$$

Consider the augmented candidate Lyapunov function:

$$V_2 = V_1 + 0.5z_2^2$$

Time derivative of  $V_2$  is the following:

$$\dot{V}_2 = \frac{z_1 z_2}{C} - c_1 z_1^2 + z_2 \dot{z}_2$$

The choice  $\frac{z_1}{C} + \dot{z}_2 = -c_2 z_2$  leads to:

$$\dot{V}_2 = -c_1 z_1^2 - c_2 z_2^2$$

If we choose  $x_3$  as a virtual control input, one has the following stabilizing function:

$$x_3^* = -z_1/C - c_2 z_2 + C \dot{x}_3^* + x_1$$

As  $x_3^*$  is not the actual control input, a new error variable,  $z_3$  between the virtual control input and its desired value  $x_3^*$ , is defined.

$$z_3 = L_1(x_3 - x_3^*) \quad (13)$$

In the same way as in step 1, dynamics of  $z_2$  and  $V_2$  can be rewritten as:

$$\dot{z}_2 = -z_1/C - c_2 z_2 + z_3/L_1$$

$$\dot{V}_2 = -c_1 z_1^2 - c_2 z_2^2 + z_2 z_3/L_1$$

**Step 3:**

The objective now is to enforce the error variables ( $z_1, z_2, z_3$ ) to vanish. To this end, let us first determine the dynamics of  $z_3$ . Deriving (13) and using (3), one obtains:

$$\dot{z}_3 = \mu_2 x_6 - x_2 - L_1 \dot{x}_3^* + r_1 x_3 \quad (14)$$

We are finally in a position to make a convenient choice of the control signal  $\mu_2$  to stabilize the whole system with state vector is ( $z_1, z_2, z_3$ ). Consider the augmented candidate Lyapunov function.

$$V_3 = V_2 + \frac{1}{2} z_3^2$$

Time derivative of  $V_3$  is given as follows

$$\dot{V}_3 = -c_1 z_1^2 - c_2 z_2^2 + z_3(\dot{z}_3 + z_2/L_1)$$

Our goal is to make  $\dot{V}_3$  to be negative definite with the following choice:

$$\dot{z}_3 + \frac{z_2}{L_1} = -c_3 z_3 \quad (15)$$

where  $c_3$  is a positive design parameter. Indeed, with this choice, the dynamics of Lyapunov function is reduced to:

$$\dot{V}_3 = -c_1 z_1^2 - c_2 z_2^2 - c_3 z_3^2$$

Combining (13) and (14) one obtained the following control law:

$$\mu_2 = 1/x_6 (-z_2/L_1 - c_3 z_3 + L_1 \dot{x}_3^* + r_1 x_3 + x_2)$$

Finally, the closed loop system is described in the ( $z_1, z_2, z_3$ ) coordinate by the following linear system:

$$\begin{pmatrix} \dot{z}_1 \\ \dot{z}_2 \\ \dot{z}_3 \end{pmatrix} = \begin{pmatrix} -c_1 & 1/C & 0 \\ -1/C & -c_2 & 1/L_1 \\ 0 & -1/L_1 & -c_3 \end{pmatrix} \begin{pmatrix} z_1 \\ z_2 \\ z_3 \end{pmatrix}$$

**B. PV voltage controller design**

The control aim is to enforce the voltage  $x_4$  across the solar panel to track a given reference voltage  $x_4^*$ . To meet this objective we use the backstepping technique for controller design and the “perturb and observe algorithm” to generate the reference voltage signal  $x_4^*$ .

**Step 1:**

Let us introduce the following current error:

$$z_4 = C_{pv}(x_4 - x_4^*)$$

where  $x_4^*$  denotes the corresponding reference signal. Using (4), time derivation of  $z_4$  yields the following error dynamics:

$$\dot{z}_4 = i_{pv} - x_5 - C_{pv} \dot{x}_4^* \quad (16)$$

If we choose  $x_5$  as the virtual control input, then the stabilizing function (17) guarantees the global stability of the subsystem (16) with respect to candidate Lyapunov function  $w_1 = \frac{1}{2} z_4^2$ .

Indeed, its time derivative is given by  $\dot{w}_1 = -c_4 z_4^2$  where  $c_4$  is a positive design parameter.

$$x_5^* = c_4 z_4 + i_{pv} - C_{pv} \dot{x}_4^* \quad (17)$$

As  $x_5^*$  is not the actual control input, we define a new error  $z_5$  between the virtual control and its desired value  $x_5^*$ .

$$z_5 = L_0(x_5 - x_5^*) \quad (18)$$

Using (17) and (18), dynamics of error  $z_4$  and Lyapunov

function  $w_1$  became:

$$\begin{aligned} \dot{z}_4 &= -c_4 z_4 - z_5 / L_0 \\ \dot{w}_1 &= -c_4 z_4^2 - z_4 z_5 / L_0 \end{aligned}$$

**Step 2:**

The objective now is to enforce the error variables ( $z_4, z_5$ ) to vanish, to this end, we determine the dynamics of  $z_5$ . Using (5) and deriving (18) one obtained:

$$\dot{z}_5 = -r_0 x_5 + x_4 - (1 - \mu_1) x_6 - L_0 \dot{x}_5^* \tag{19}$$

We considered the augmented Lyapunov function candidate

$$w_2 = w_1 + \frac{1}{2} z_5^2$$

The time derivative of  $w_2$  is given as follows:

$$\dot{w}_2 = C_4 z_4^2 + z_5 (\dot{z}_5 - \frac{z_4}{L_0})$$

we put:  $-c_5 z_5 = -\frac{z_4}{L_0} + \dot{z}_5$  (20)

where  $c_5$  is a positive design parameter. Indeed, with this choice, the dynamics of Lyapunov function is reduced to:

$$\dot{w}_2 = -c_4 z_4^2 - c_5 z_5^2$$

Combining (19) and (20) one obtained the following control law:

$$\mu_1 = 1 - 1/x_6 (-r_0 x_5 + x_4 - z_4/L_0 + c_5 z_5 + L_0 \dot{x}_5^*)$$

Closed loop behavior of the subsystem under study is given as follows:

$$\begin{pmatrix} \dot{z}_4 \\ \dot{z}_5 \end{pmatrix} = \begin{pmatrix} -c_4 & -1/L_0 \\ 1/L_0 & -c_2 \end{pmatrix} \begin{pmatrix} z_4 \\ z_5 \end{pmatrix}$$

**C. Generation of the reference voltage**

To ensure the correct operation of PV module at its maximum power point as the temperature, insolation and load vary, we use well known ‘‘perturb and observe algorithm (P&O). P&O is the most method used due to its simplicity and a fewer measured parameter, it has two input signals. They are, the PV voltage and the current, and one output signal which is a voltage reference that must be applied to the regulator. The algorithm steps are described as shown in the following flowchart [14].

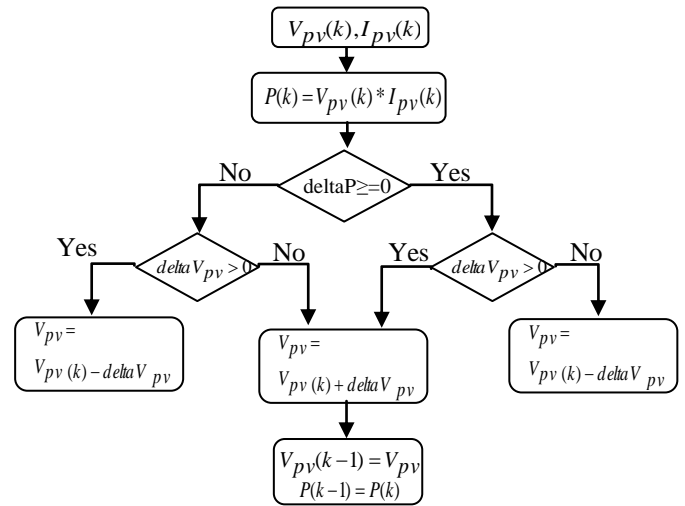


Fig.6: P&O flowchart

**D. DC link voltage regulation**

To achieve the PFC, it is necessary to control DC link voltage to track its desired voltage reference, to do that, a simple PI regulator is required.

PI transfer function is:

$$F(s) = k_1 \frac{(1 + \tau_1 s)}{\tau_1 s}$$

**V. SIMULATION RESULTS**

In this section the controller that has been designed in the above section will be tested in the SimPower/Simulink/Matlab environment with the following system characteristics:  $L_0 = 0.3H$ ;  $r_0 = 0.05\Omega$ ;  $C_{pv} = 0.2mF$ ,  $L_1 = 2mH$ ;  $L_g = 2mH$ ;  $r_1 = 5m\Omega$ ;  $r_g = 5m\Omega$ ;  $C = 5mF$ .

The following values of the controllers design parameters proved to be suitable:  $c_1 = 10000$ ,  $c_2 = 440$ ,  $c_3 = 290$ ,  $c_4 = 8000$ ,  $c_5 = 90000$ ,  $F_p = 10KHz$ ,  $\tau_1 = 25ms$ ,  $k_1 = 0.5$ .

The reference DC link voltage is fixed to 300 V.

Figures 6.a-d shows some simulation results studies, which are selected to demonstrate the most significant aspects of the grid-connected system behavior. The simulation results have been obtained under standard climatic conditions (1000 W/m<sup>2</sup> and 25°C). The figures illustrate the response of the grid-connected PV system in standard climatic conditions. It can be clearly seen that, in steady state, the PV generator provides the maximal power, which is equal to 880 W. Figure 6.a presents the evolution the injected current in the grid. Figure 6.b shows the PV voltage with its reference generated by the ‘‘P&O’’ algorithm. Figure 6.c show the DC link voltage regulation is guaranteed. Figure 6d shows that the current and the grid voltage are in phase, and sinusoidal. As a result, a unit power factor is achieved.

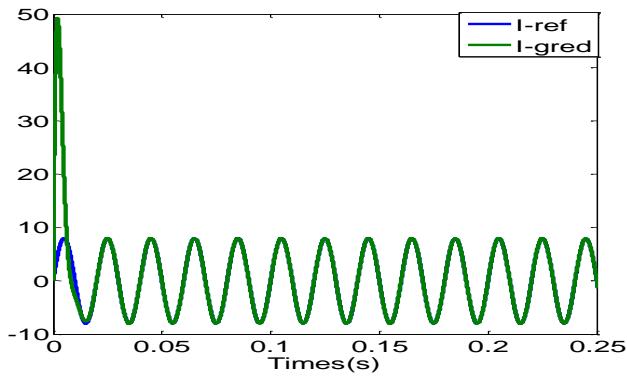


Fig.6.a: injected current with its reference

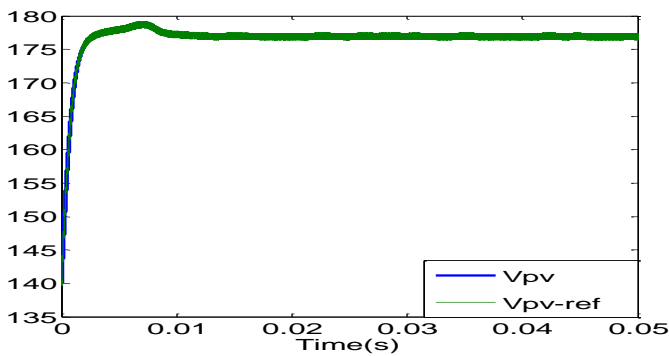


Fig.6.b: PV voltage with its reference

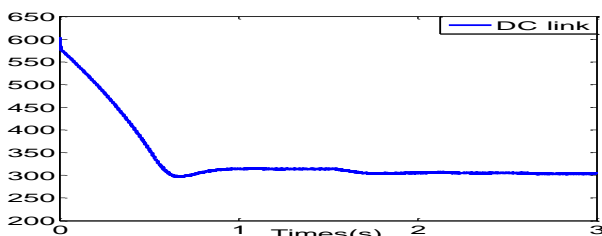


Fig.6.c: DC link voltage

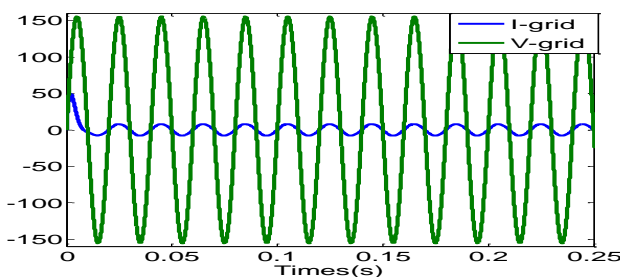


Fig.6.d: PFC checking

## VI. CONCLUSION

In this paper an advanced controller is developed for PV grid connected system. The later is described by 6<sup>th</sup> order

nonlinear averaged model. The controller design is made based on backstepping technique and Lyapunov stability. Simulations under Matlab/Simulink prove that the controller meet the performances, for which it was designed, namely: i) Global asymptotic stability of the all system ii) Perfect power factor in the grid iii) Maximum power point tracking.

## REFERENCES

- [1] N. Femia, G. Petrone, G. Spagnuolo and, M. Vitelli, "Optimization of perturb and observe maximum power point tracking method," IEEE Trans Power Electron 2005; vol. 20(4): pp. 963–73.
- [2] K. Soon Tey, S. Mekhilef , "Modified incremental conductance MPPT algorithm to mitigate inaccurate responses under fast-changing solar irradiation level," ScienceDirect, Solar Energy, Vol. 101, March 2014, pp 333-342.
- [3] A.F. Okou, O. Akhrif, R. Beguenane, M. Tarbouchi " Nonlinear Control Strategy Insuring Contribution Of PV Generator to Voltage and Frequency Regulation". Power Electronics, Machines and Drives, 27-29 March 2012, pp. 1-5.
- [4] Adrian V. Timbus, M. Ciobotaru, R. Teodorescu and F. Blaabjerg, " Adaptive Resonant Controller for Grid-Connected Converters in Distributed Power Generation Systems". Applied Power Electronics Conference and Exposition, 19-23 March 2006.
- [5] S. Dasgupta, S. K. Sahoo, S. K. Panda, Senior, "A New control strategy for Single Phase Series Connected PV Module Inverter for Grid Voltage Compensation". Power Electronics and Drive Systems, 2-5 Nov. 2009, pp: 1317-1322.
- [6] M. Ciobotaru, R. Teodorescu and F. Blaabjerg, "Control of single-stage single-phase PV inverter". Power Electronics and Applications, 2005 European Conference.
- [7] Tofighi, A., Kalantar, M.. "Power management of PV/battery hybrid power source via passivity-based control", Renew. Energy, 2011, 36, pp. 2440-2450.
- [8] E. M. Natsheh, A. R. Natsheh, A. Albarbar, "Intelligent controller for managing power flow within standalone hybrid power systems", IET Sci. Meas. Technol., 2013, Vol. 7, Iss. 4, pp. 191-200.
- [9] H. Cha, T. K. Vu and J. E. Kim, "Design and Control of Proportional-Resonant Controller Based Photovoltaic Power Conditioning System". Energy Conversion Congress and Exposition , pp. 2198-2205, IEEE 20-24 Sept. 2009.
- [10] M.G. Villava, J. R. Gazoli, E.F. Ruppert , " Modeling and circuit-based simulation of photovoltaic array," Brazilian journal of power electronics, Vol. 14, pp. 35-45, 2009.
- [11] P. Yadav, B. Tripathia, K. Pandey, M. Kumar, "Effect of varying concentration and temperature on steady and dynamic parameters of low concentration photovoltaic energy system". International Journal of Electrical Power & Energy Systems.
- [12] H. Tian, F.Mancilla-Davida, K. Ellisd, E. Muljadid, P. Jenkinsd, "A cell-to-module-to-array detailed model for photovoltaic panels". Solar Energy, Vol. 86, Iss. 9, pp 2695-2706, Sept. 2012.
- [13] H. Poor, "An Introduction to Signal Detection and Estimation". New York: Springer-Verlag, 1985, ch. 4.
- [14] B. Bhandari , S. Poudel, Kyung-Tae Lee, Sung-Hoon Ahn, "Mathematical Modeling of Hybrid Renewable Energy System: A Review on Small Hydro-Solar-Wind Power Generation", International Journal of Precision Engineering and Manufacturing-Green Technology, Vol. 1, Iss. 2, pp 157-173, April 2014.